Quantitative real-time RT-PCR analysis

The cDNA was used as a template for individual PCR reactions using exon skipping specific primer sets (Supplementary Table S11), which were designed using the Primer Express program (Applied Biosystems, Foster City, CA, USA) and Primer3 program. PCR reactions were conducted using SYBRGreen Real-time PCR Master Mix (TOYOBO) according to the manufacturer's instructions, except that the annealing time was reduced to 15 s. The quantitative PCR analysis was performed using the StepOnePlus device (Applied Biosystems). Amplification specificity was verified by visualizing the PCR products on an ethidium bromide-stained 2% agarose gel. GAPDH was used to normalize the expression data.

Ultraviolet (UV) melting experiment

UV melting experiments were conducted using a Shimadzu UV-1650PC UV-Vis spectrophotometer equipped with a T_m analysis accessory TMSPC-8 (Shimadzu, Kyoto, Japan). Equimolecular amounts of SSO and complementary RNA oligonucleotide were dissolved in 10 mM sodium phosphate buffer (pH 7.2) containing 10 mM NaCl to give a final strand concentration of 2.0 μM. The samples were boiled for 3 min, followed by slow cooling to room temperature. The absorption was recorded at 260 nm in the forward and reverse direction from 5°C to 95°C at a scan rate of 0.5°C/min. The first derivative was calculated from the smoothed UV melting profile. The peak temperatures in the derivative curve were designated as the melting temperature, T_m.

In silico analysis to search for target sequence

To know the number of genes that contain the sequence perfectly matched to the target sequence of AONs, we used GGRNA, a Google-like fast search engine for genes and transcripts (http://GGRNA.dbcls.jp/) (35). In this analysis, we considered splicing variants with the same gene ID as one gene and excluded the genes which do not encode proteins.

RESULTS

Screening for LNA SSOs effective for inducing exon skipping

We performed a screening analysis to obtain effective LNA SSOs that induced skipping of exon 58 of the human dystrophin gene. Prior to starting the screening of the SSOs, we developed a minigene reporter plasmid containing exons 57–59 of the human dystrophin gene. Subsequently, we established a stable reporter cell line in which the reporter plasmid was incorporated into the genomic DNA and used as a splicing assay system. To evaluate the efficacy of the designed SSOs, the reporter cells were transfected with each SSO, and exon skipping was analyzed by RT-PCR (Supplementary Figure S1).

In this screening study, we designed a series of 15-mer LNA/DNA mixmers with a LNA substitution at every third nucleotide position. These mixmers contained five LNA units in the SSO sequence, in which the phosphodiester linkages were completely replaced by PS linkages (Figure 1). To prevent RNase H-dependent RNA degradation, we designed the number of continuous natural nucleotides in the SSO to be less than two (Figure 2A) (36). The screening was composed of three steps. At the first step, nine non-overlapping LNA SSOs were designed to tile across the entire target exon 58 sequence to detect a prospective target site (Figure 2B and Supplementary Table S1). Reporter cells were transfected with 100 nM SSOs for 24 h. Total RNA samples were prepared, and RT-PCR analyses showed that three LNA SSOs, i.e. -5+10, +70+84 and +115-8, were effective in slightly inducing exon skipping of exon 58 (the rate of exon skipping was 10%–20%) (Figure 2C and Supplementary Figure S2A).

In the second step, to detect the more active SSOs, we synthesized three sets of 15-mer LNA SSOs shifted by three bases around each expected target sequence, i.e. -5+10, +70+84 and +115-8 (Figure 2D and Supplementary Table S2). These SSOs (100 nM) were transfected into the reporter cell line, and total RNA samples were prepared after a further 24 h incubation. The RT-PCR results suggested that both the 5′ and 3′ splice sites in addition to the 27-base region from +70 to +96 of exon 58 are hot spots for inducing exon skipping (Figure 2E and Supplementary Figure S2B). In addition, this region was predicted as an exonic splicing enhance (ESE) site by ESEfinder3.0 (Supplementary Figure S3) (37,38). In this case, we decided to select two SSOs, -2+13 and +106+120, as templates for the next screening step given their high ability to modulate splicing (the rate of exon skipping increased to ca. 50%) (Supplementary Figure S2B).

Finally, we designed a further four LNA SSOs shifted by one nucleotide around each SSO, i.e. -2+13 and +106+120 (Figure 2F and Supplementary Table S3). In the third step, we assessed the expression of exon 58-skipped mRNA by means of quantitative real-time RT-PCR to rigorously evaluate the abilities of the SSOs. Both the SSO (-1+14) in the 5′ splice site and the SSO (+108-1) in the 3′ splice site showed higher exon 58 skipping activity (Figure 2G). Surprisingly, in some cases SSOs that are frameshifted by one nucleotide resulted in loss of SSO activity (e.g. -4+11 versus -3+12). These findings demonstrate that exon 58 skipping can be modulated by 15-mer LNA/DNA mixmer SSOs targeting near the 5′ and 3′-splice sites of exon 58, and that this activity is strongly dependent on the target sequence.

Evaluation of the effect of number of LNAs and T_m value on splicing

In the following experiments, we selected two sequences identified from the above screening for exon skipping (-1+14 and +108-1). To investigate the relationship between the number of LNAs in the sequence of the SSOs and skipping activity, we synthesized a series of 15-mer SSOs that had various numbers of LNAs (Figure 3A). To protect the SSOs against nuclease degradation and prevent RNase H-induced pre-mRNA digestion, 2′-OMe RNAs were introduced into SSOs if fewer than five LNAs were in the sequence. We determined the T_m values of these SSOs with complementary RNA by UV melting experiments per-

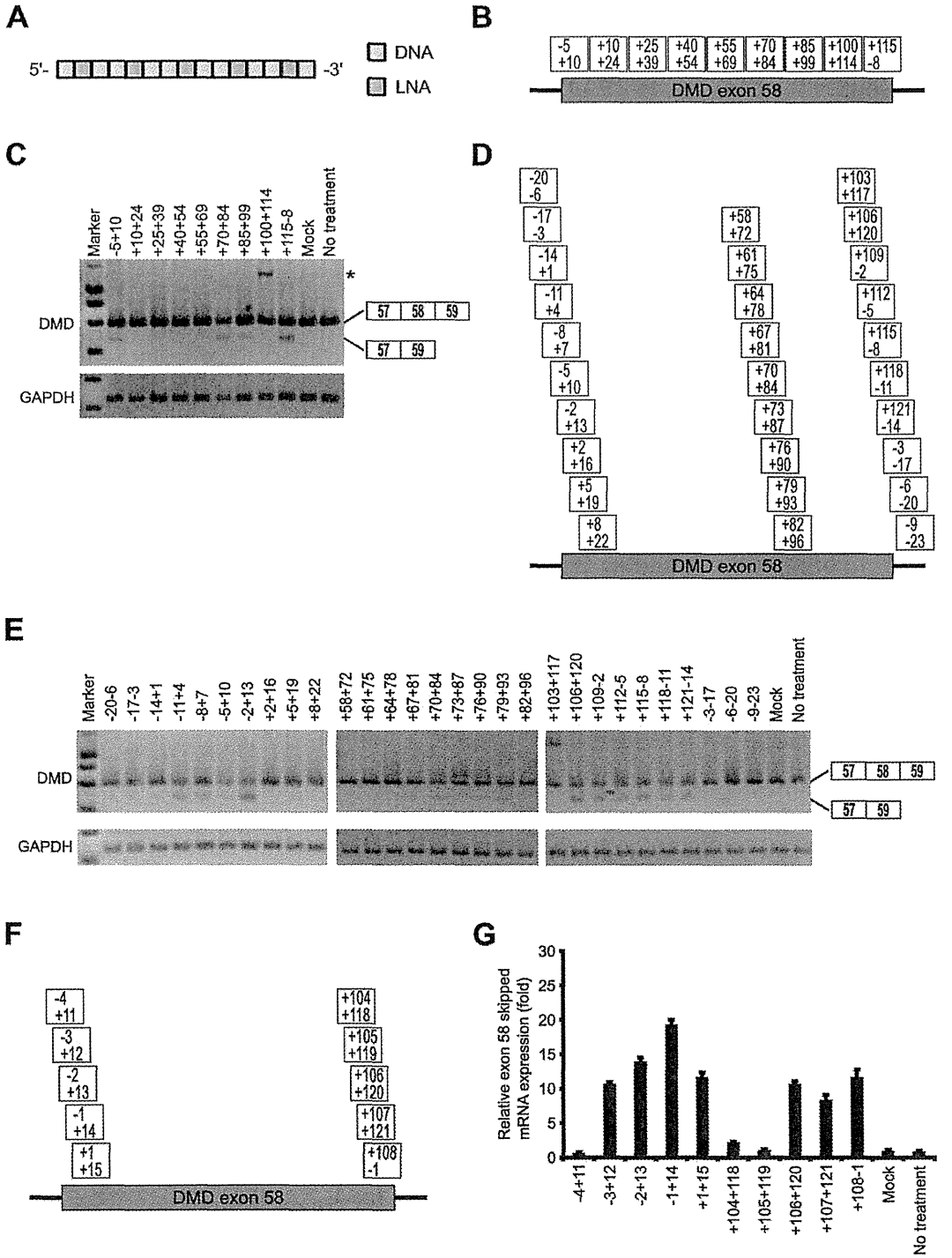

Figure 2. Screening of 15-mer LNA/DNA mixmer SSOs designed to induce dystrophin exon 58 skipping. (**A**) Schematic representation of the position of LNA in the 15-mer SSO used in this screening. Each box represents one nucleotide; the blue box and yellow box indicate LNA and DNA, respectively. (**B, D, F**) Annealing sites of SSOs targeted to dystrophin exon 58 are indicated by the boxes for the first (B), second (D) and third screening (F). (**C, E**) The reporter cells were transfected with the indicated LNA/DNA mixmer SSOs (100 nM) for 24 h. RT-PCR analyses showing the full-length upper band (587 bp) and the skipped lower band (466 bp). The band marked by an asterisk represents an intron 58 inclusion product. GAPDH was used as an internal control. (C) and (E) express the results of the first and second screening, respectively. (**G**) The levels of exon 58-skipped mRNA fragments were measured by quantitative real-time RT-PCR and normalized against the signal of GAPDH mRNA, relative to the value in the mock set as 1. Values represent the mean ± standard deviation of triplicate samples. Reproducible results were obtained from two independent experiments. Mock: treated with Lipofectamine only; no treatment: no transfection.

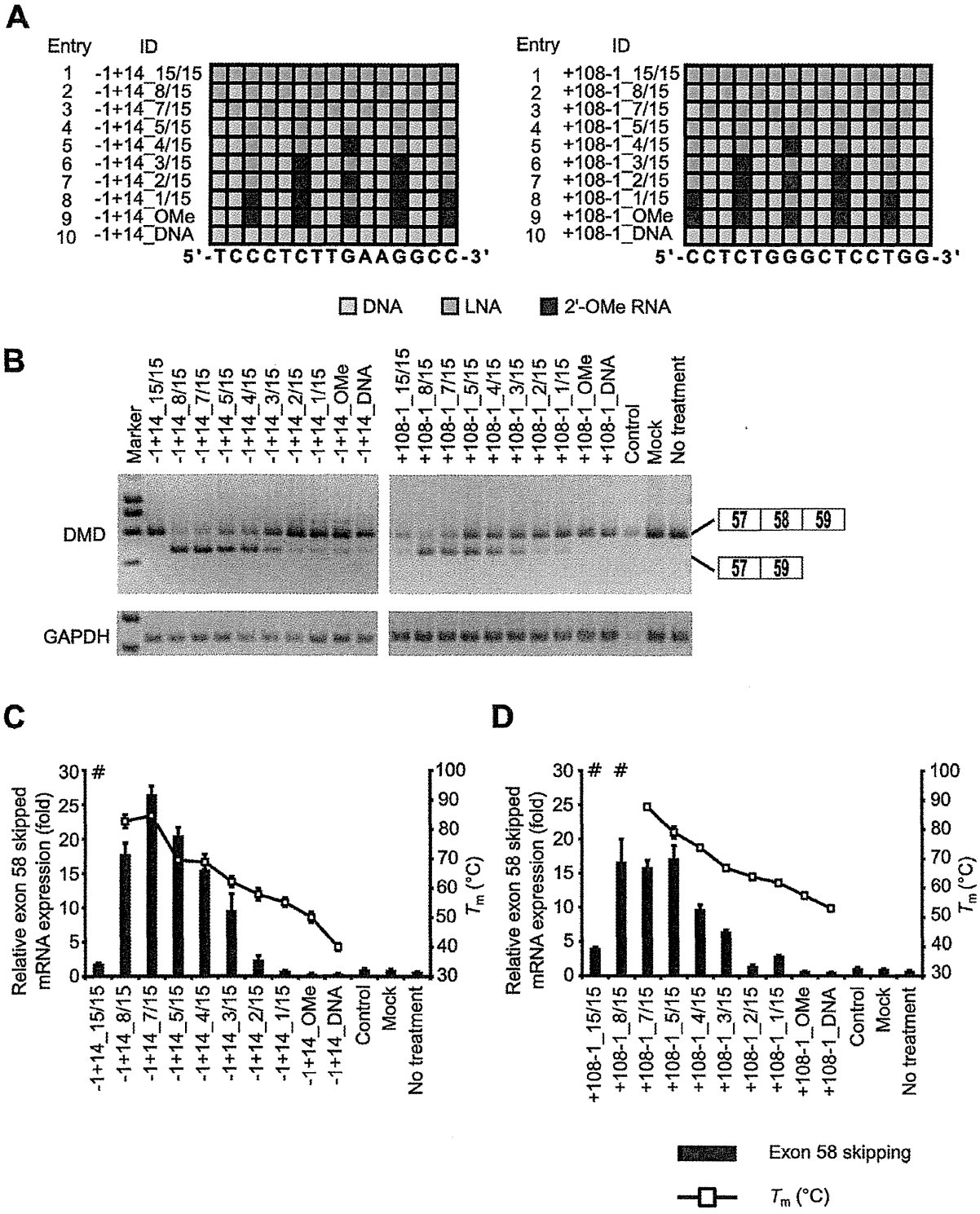

Figure 3. Evaluation of exon skipping activity of 15-mer SSOs with various numbers of LNAs and T_m values. (**A**) Schematic representation of the position of LNA in the 15-mer SSOs used in this study. Each box represents one nucleotide; the blue box, red box and yellow box indicate LNA, 2′-OMe RNA and DNA, respectively. (**B**) The reporter cells were transfected with the indicated LNA/DNA mixmer SSOs (30 nM) for 24 h. RT-PCR analyses were performed as described in Figure 2C. LNA SSO (+10+24), which showed no exon skipping effects, was used as a control. (**C** and **D**) The levels of exon 58-skipped mRNA fragments were measured by quantitative real-time RT-PCR (for details see Materials and Methods and Figure 2G). Values represent the mean ± standard deviation of triplicate samples. Reproducible results were obtained from two independent experiments. The T_m of each SSO with a complementary RNA under low-sodium conditions is also shown. # indicates that no sigmoidal melting curve was observed, even at higher T_m values. The data are the mean ± standard deviation ($n = 4$). (C) and (D) express exon skipping results of using SSOs targeted the 5′ and 3′ splice sites, respectively.

formed under low-sodium conditions (10 mM phosphate buffer (pH 7.2) containing 10 mM NaCl) (Supplementary Tables S4 and S5). The lower ionic concentration of the solvent tended to decrease T_m relative to the typical ionic concentrations, such as 100 mM NaCl (Supplementary Table S4). LNA SSO (+10+24) did not show an exon skipping effect (Figure 2C) and was thus used as a control.

We transfected reporter cells with 30 nM SSOs, and the cells were then incubated for 24 h. Then, total RNA samples were prepared, and exon 58-skipped mRNA levels were determined by both RT-PCR and quantitative real-time RT-PCR. RT-PCR analysis indicated that increasing the number of LNAs enhanced exon skipping activity (the rate of exon skipping reached 80%) (Figure 3B and Supplementary Figure S4A and B). Similar results were obtained by quantitative real-time RT-PCR assays, and SSOs containing between five and eight LNAs induced exon skipping at high levels (Figure 3C and D). On the other hand, SSOs fully modified with LNA showed very low activity, and their T_m values were higher than 95°C. In our experiments, efficient exon skipping activity was obtained when LNA/DNA mixmer SSOs were designed with a T_m in the range of 60°C–90°C (low sodium conditions). In comparison to the LNA SSOs, both the 2′-OMe SSO and DNA SSO hardly affected exon skipping. These results indicate that the number of LNA in the SSO sequence and the T_m of the SSOs play important roles in exon skipping.

Influence of SSO length on exon skipping

To determine whether the SSO length affects splicing modulation, we tested SSOs targeting the 3′ splice site. The length of the SSOs ranged from 9 to 23 nucleotides. Taking into account the T_m values of the short SSOs, we designed eight SSOs that contained 50% LNAs in their sequences (Figure 4A and Supplementary Table S6). We also determined dissociation constant (K_d) for LNA/DNA mixmer SSOs to mRNA (Supplementary Materials and Methods and Supplementary Table S6).

Reporter cells were transfected with 30 nM SSOs. Total RNA samples were prepared after a further 24 h incubation, and we assessed the expression of exon 58-skipped mRNA by means of RT-PCR and quantitative real-time RT-PCR. RT-PCR revealed that the longer LNA SSOs induced exon skipping with high efficiency (the rate of exon skipping was ~75%) (Figure 4B and Supplementary Figure S5). Intriguingly, when the levels of exon 58-skipped mRNA were analyzed by quantitative real-time RT-PCR, the 13-mer SSO (+110-1_6/13) produced high amounts of exon 58 skipping mRNAs in a concentration-dependent manner (Figure 4C–E and Supplementary Figure S6A). A concentration-dependent increase was also observed for other SSO (-1+14_7/15) targeting the 5′ splice site (Supplementary Figure S6B–D). Amazingly, the 9-mer LNA SSO (+114-1_4/9) (T_m = 66.7°C) induced exon skipping, in a similar manner as 19-, 21- and 23-mer SSOs (Figure 4C).

Characterization of 9-mer LNA SSOs

Although no reports to date have indicated that 9-mer SSOs induce exon skipping, we found that even a 9-mer SSO (+114-1_4/9) (four LNA and five DNA) could modulate splicing, albeit weakly. Therefore, to further improve the efficiency of exon skipping, we designed another two 9-mer SSOs containing seven LNAs having the same sequence as +114-1_4/9 (Figure 5A and Supplementary Table S7). As expected, the T_m values of both SSOs (+114-1_7/9_1 and +114-1_7/9_2) were higher than that of SSO (+114-1_4/9) (87.1°C, 83.1°C, and 66.7°C, respectively) (Supplementary Table S7).

The reporter cells were treated with 30 nM SSOs for 24 h and then subsequently lysed with the total RNA extracted. Interestingly, 9-mer LNA SSO (+114-1_7/9_2) presented 1.5-fold higher activity than the other 9-mer LNA SSOs (Figure 5B and C and Supplementary Figure S7). It seems that the position of LNA analogues in the SSO sequence may be a key factor for exon skipping. Moreover, this 9-mer SSO induced exon skipping in a concentration-dependent manner (Figure 5D and Supplementary Figure S8A–E). In contrast, the 9-mer 2′-OMe SSO (T_m = 40.0°C) exhibited no exon skipping activity at all. In this study, we report for the first time that 9-mer LNA SSOs have sufficient activity to induce exon skipping.

Short 7-mer LNA SSO-induced exon skipping in the reporter cells

To determine the minimum length of LNA SSO required for inducing exon skipping, we tested short LNA SSOs (6- to 9-mer) containing various numbers of LNAs (Supplementary Table S8). We designed three sets of LNA SSOs (fully modified LNA SSOs which have as high T_m value as possible, LNA/DNA mixmer SSOs containing 50% LNAs, such as Figure 4A, and LNA/DNA mixmer SSOs containing two DNAs like a +114-1_7/9_2, respectively) for each length (Figure 6A).

Reporter cells were transfected with 30 nM SSOs. Total RNA samples were prepared after a further 24 h incubation, and we assessed the expression of exon 58-skipped mRNA by means of RT-PCR and quantitative real-time RT-PCR. RT-PCR revealed that 9-, 8- and 7-mer LNA SSOs induced exon skipping, while 6-mer LNA SSOs did not show any activity (Figure 6B and Supplementary Figure S9). In the case of short LNA SSOs, the longer SSOs tend to have higher activity and exon skipping activity was obtained when LNA SSOs were designed with a T_m higher than 60°C (low sodium conditions) (Figure 6C). These results indicate that even very short 7-mer LNA SSO provides exon skipping activity.

Effect of mismatches on exon skipping activity and sequence specificity

To assess the specificity of LNA SSOs, we introduced one, two or three mismatches in both 13- and 9-mer LNA SSOs (Figure 7A and B and Supplementary Table S9). The reporter cells were transfected with 30 nM LNA SSOs. Twenty-four hours after transfection, total RNAs were extracted and the expression levels of exon 58-skipped mRNA were analyzed by both RT-PCR and quantitative real-time RT-PCR (Figure 7C and D and Supplementary Figure S10). We observed that when one LNA mismatch is introduced into 13-mer LNA SSO (six LNA and seven DNA)

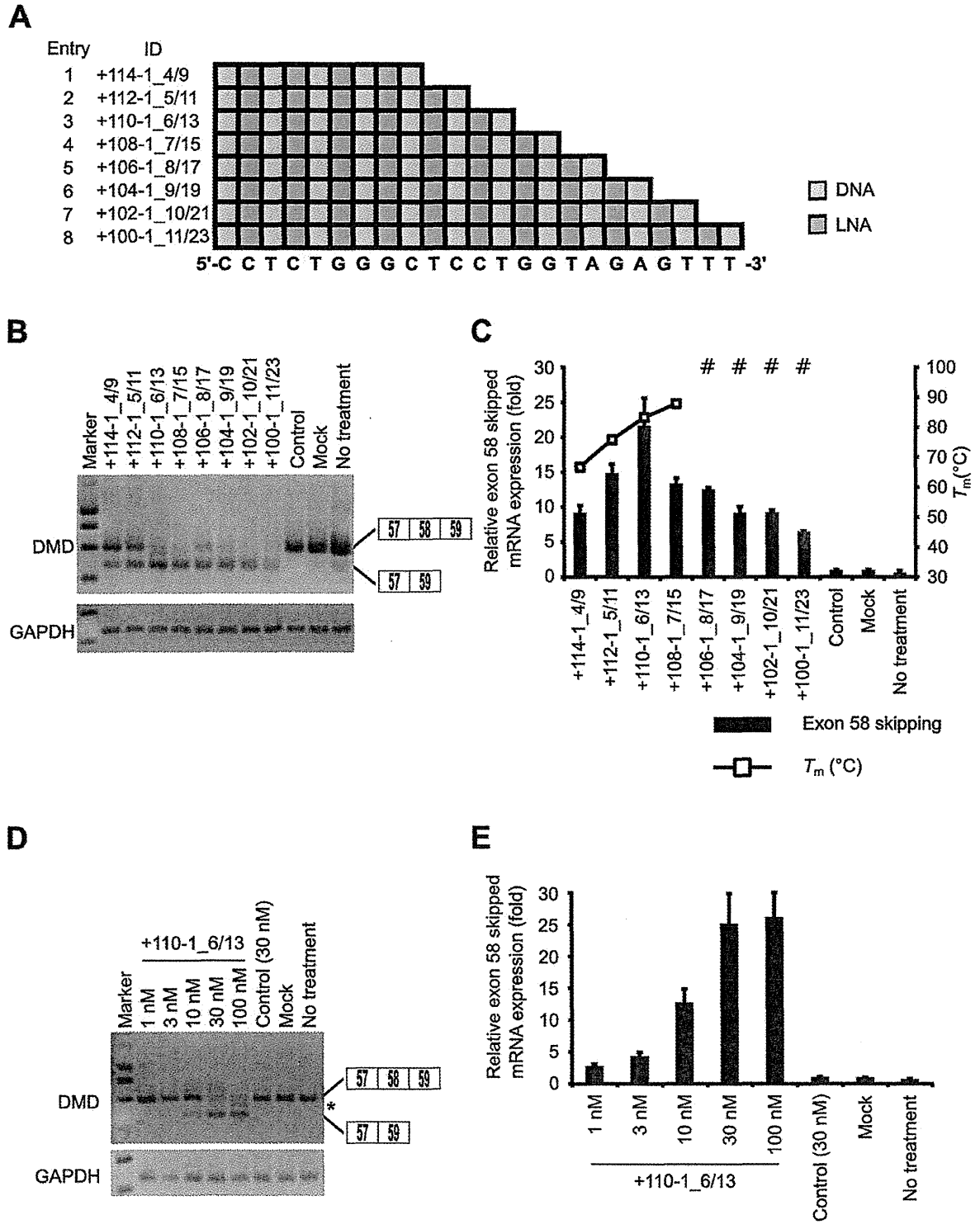

Figure 4. Comparison of the exon skipping activity of various lengths of LNA/DNA mixmer SSOs. (**A**) Schematic representation of the position of LNA in the SSOs used in this study. (**B** and **D**) The reporter cells were transfected with the indicated LNA/DNA mixmer SSOs (30 nM (B) or various concentrations (1–100 nM) (D)) for 24 h. RT-PCR analyses were performed as described in Figure 3B. The band marked by an asterisk represents a partial intron 58 inclusion product. (**C** and **E**) The levels of exon 58-skipped mRNA fragments were measured by quantitative real-time RT-PCR (for details see Materials and Methods and Figure 2G). Values represent the mean ± standard deviation of triplicate samples. Reproducible results were obtained from two independent experiments. The T_m of each SSO with a complementary RNA under low-sodium conditions is determined as described in Figure 3C. The data are the mean ± standard deviation ($n = 4$).

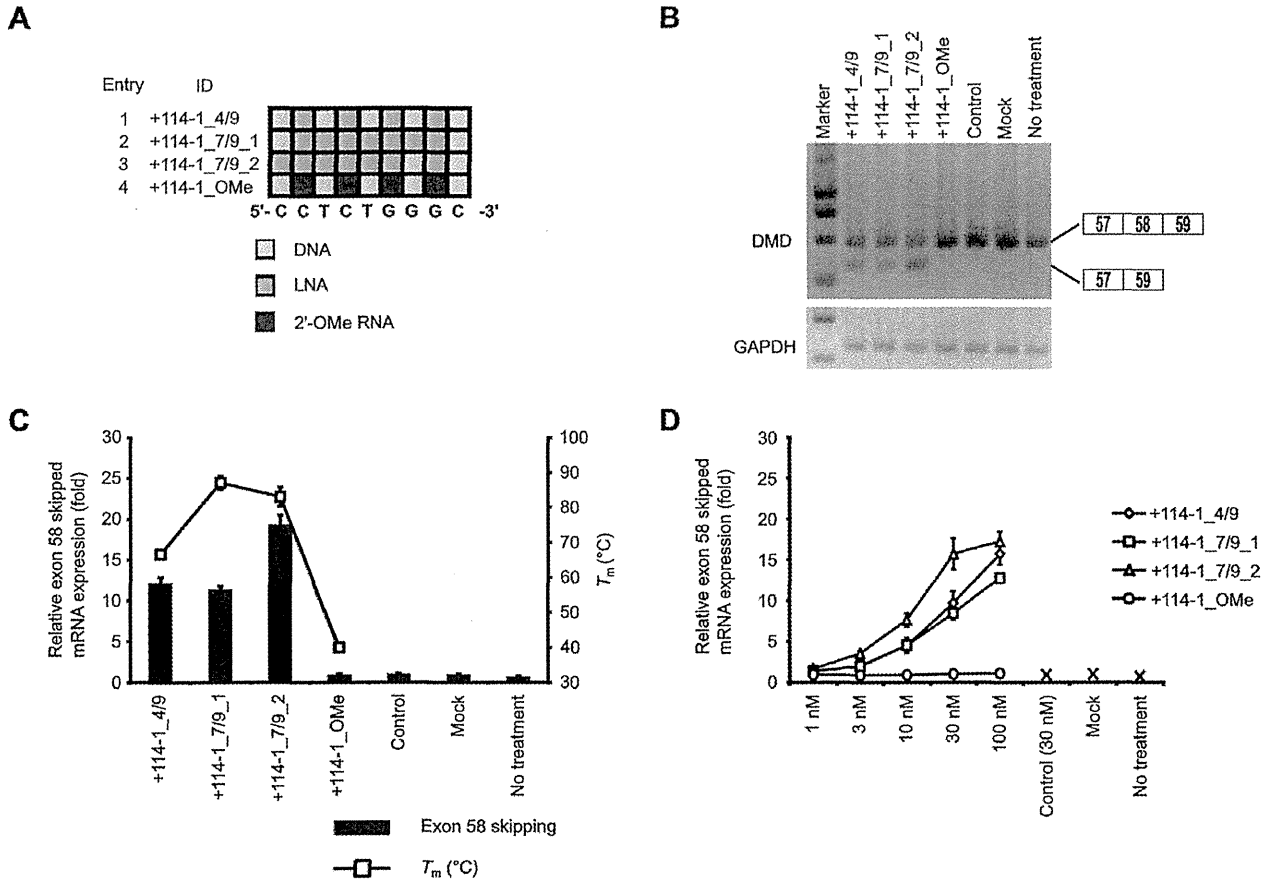

Figure 5. Exon skipping activity of 9-mer LNA/DNA mixmer SSOs. (**A**) Schematic representation of the position of LNA in the 9-mer SSOs used in this study. (**B**) The reporter cells were transfected with the indicated LNA/DNA mixmer SSOs (30 nM) for 24 h. RT-PCR analyses were performed as described in Figure 3B. (**C** and **D**) Quantitative real-time RT-PCR analyses of RNA samples from reporter cells treated with SSOs at 30 nM (C) or at various concentrations (1–100 nM) (D) for 24 h were performed as described in Figure 2G. Values represent the mean ± standard deviation of triplicate samples. Reproducible results were obtained from two independent experiments. The T_m of each SSO with a complementary RNA under low-sodium conditions is also shown. The data are the mean ± standard deviation ($n = 4$).

(+110-1_G117A, +110-1_G117C and +110-1_G117T), they can still induce exon skipping of exon 58. In contrast, mismatched LNA SSOs with two or three mismatches (+110-1_G115C/G117C and +110-1_G115C/g116c/G117C) did not show exon skipping activity. In the case of 9-mer LNA SSO (seven LNA and two DNA), one to three LNA mismatches abrogated the effect on exon 58 skipping. These results indicate that a 9-mer LNA SSO shows a better mismatch discrimination than a 13-mer LNA SSO. We next searched for target sequence of both 13- and 9-mer LNA SSOs using GGRNA (35). It is revealed that there were 914 genes that have perfect match with the 9-mer LNA SSO (+114-1_7/9_2). On the other hand, only 8 genes contain sequences perfectly matched to the 13-mer LNA SSO (+110-1_6/13) (Table 1). Thus, although 9-mer LNA SSOs improve mismatch discrimination in comparison with 13-mer LNA SSOs, 9-mer SSOs may be too short to target unique sites.

Induction of exon 58 skipping of endogenous human dystrophin transcript by using LNA SSO

Finally, to examine whether LNA SSOs modulate the splicing of endogenous human dystrophin transcript, we used primary HSMM cells. Cells were treated with the differentiation medium 24 h prior to transfection. Then, HSMM cells were transfected with 500 nM SSOs. Total RNA samples were prepared after a further 24 h incubation, and we assessed the expression of exon 58-skipped endogenous human dystrophin mRNA by means of RT-PCR. Although the 9-mer LNA SSO (+114-1_7/9_2) induced weak exon skipping, the 13-mer LNA SSO (+110-1_6/13) induced a high amount of exon skipping (Figure 8). In contrast, control SSO did not affected exon skipping. These data indicate that LNA SSOs are able to induce exon skipping of endogenous human dystrophin in cultured muscle cells.

DISCUSSION

In this study, we designed and evaluated the exon skipping ability of a series of LNA SSOs complementary to the hu-

Table 1. A number of genes that contain the sequence complementary to each AON. Sequences are shown from 5′ to 3′.

ID	Target sequence	Length (bp)	No. of genes containing the target sequence
+114-1_7/9_2	GCCCAGAGG	9	914
+110-1_6/13	AGGAGCCCAGAGG	13	8

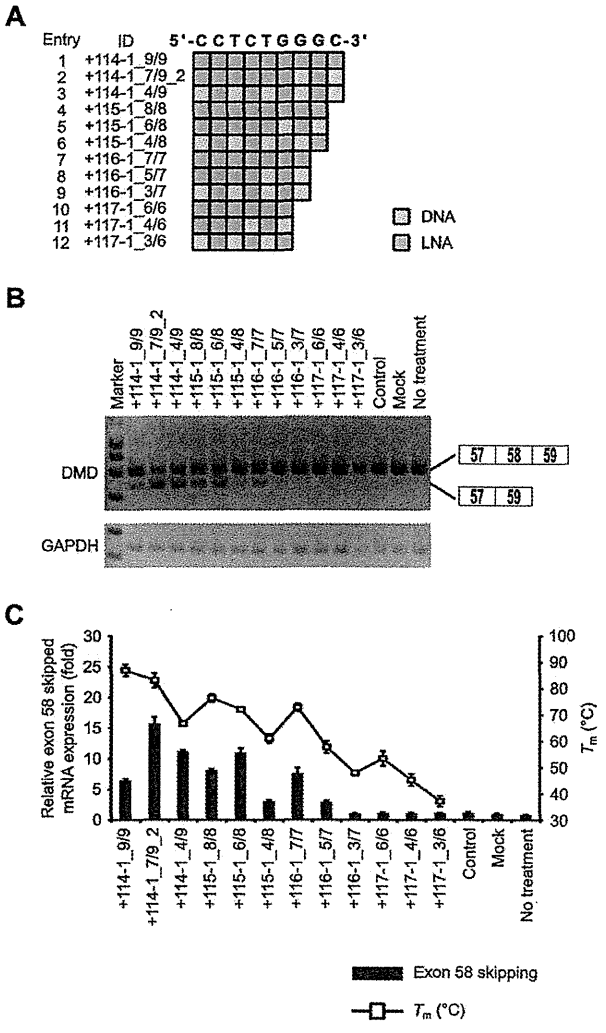

Figure 6. Comparison of exon skipping activity of short (6- to 9-mer) LNA SSOs. (**A**) Schematic representation of the position of LNA in the SSOs used in this study. (**B**) The reporter cells were transfected with the indicated LNA/DNA mixmer SSOs (30 nM) for 24 h. RT-PCR analyses were performed as described in Figure 3B. (**C**) The levels of exon 58-skipped mRNA fragments were measured by quantitative real-time RT-PCR (for details see Materials and Methods and Figure 2G). Values represent the mean ± standard deviation of triplicate samples. Reproducible results were obtained from two independent experiments. The T_m of each SSO with a complementary RNA under low-sodium conditions is also shown. The data are the mean ± standard deviation ($n = 3$–4).

man dystrophin exon 58 sequence. We also indicated that LNA SSOs induce endogenous dystrophin exon 58 skipping in primary human skeletal muscle cells.

To develop the splicing assay system we used native human dystrophin sequences because it is thought that the RNA structures play an important role in the regulation of splicing (39). According to previous reports, exon skipping target to exon 58 is applicable to only 0.1% of DMD patients (40). The average length of human dystrophin introns tends to be higher than 25 000 bp; therefore, the entire gene is inappropriate to introduce into a plasmid. However, intron 58, whose length is only 608 bp, has a much shorter sequence than other introns (41). We therefore selected exon 58 to construct our assay system despite the rarity of patients with mutations correctable by exon 58 skipping. On the other hand, the intron 57 sequence, consisting of 17 684 bp, is too long to insert into a reporter plasmid. Thus, although splicing regulatory sequences are located not only near exon–intron junctions but also intronic regions, we decided to use the human dystrophin minigene encompassing exons 57–59 by removing the sequence of intron 57 from position +207 to +17 486. Moreover, we established a stable Flp-In 293 cell line in which the reporter plasmid is incorporated into the genomic DNA, and that this screening cell line is easier to maintain than primary cells due to the robust growth. Because LNA SSOs selected by using this screeing cell line induced exon 58 skipping of endogenous dystrophin gene in the HSMM (Figure 8), this cell line is a useful evaluation tool for screening a lot of SSOs, as used in this study.

First, to identify effective SSOs capable of modulating exon skipping, 43 LNA SSOs, each with a length of 15 bases, were evaluated by RT-PCR. Exon skipping was induced at high levels by targeting either acceptor or donor sites with SSOs (Figure 2). In addition, this systematic screen also identified the 27-bp region from +70 to +96 of exon 58 as an appropriate target for SSOs. Interestingly, this region was predicted to be an ESE site by ESEfinder3.0 (Supplementary Figure S3) (37,38). This result was in agreement with previous studies using other chemically modified SSOs (42,43,44). Thus, splicing acceptor sites, splicing donor sites and ESE motifs are good targets for modulating exon splicing by LNA SSOs.

Second, we showed that exon skipping activity is dependent on the number of LNAs in the sequence of SSOs. Among the 15-mer mixmer SSOs, SSOs containing between five and eight LNA units showed especially high activity, and there was a correlation between their activity and the T_m of the SSOs with complementary RNA (Figure 3). In comparison to the LNA SSOs, the 2′-OMe SSO (five 2′-OMe and ten DNA) scarcely produced exon skipping (Figure 3), possibly because the exon skipping activity may be related to the binding affinity of each analogue. LNA-based oligonucleotides significantly enhanced hybridization to the complementary RNA, and the T_m was increased by 2°C–8°C for each LNA nucleotide incorporated (45,46), whereas

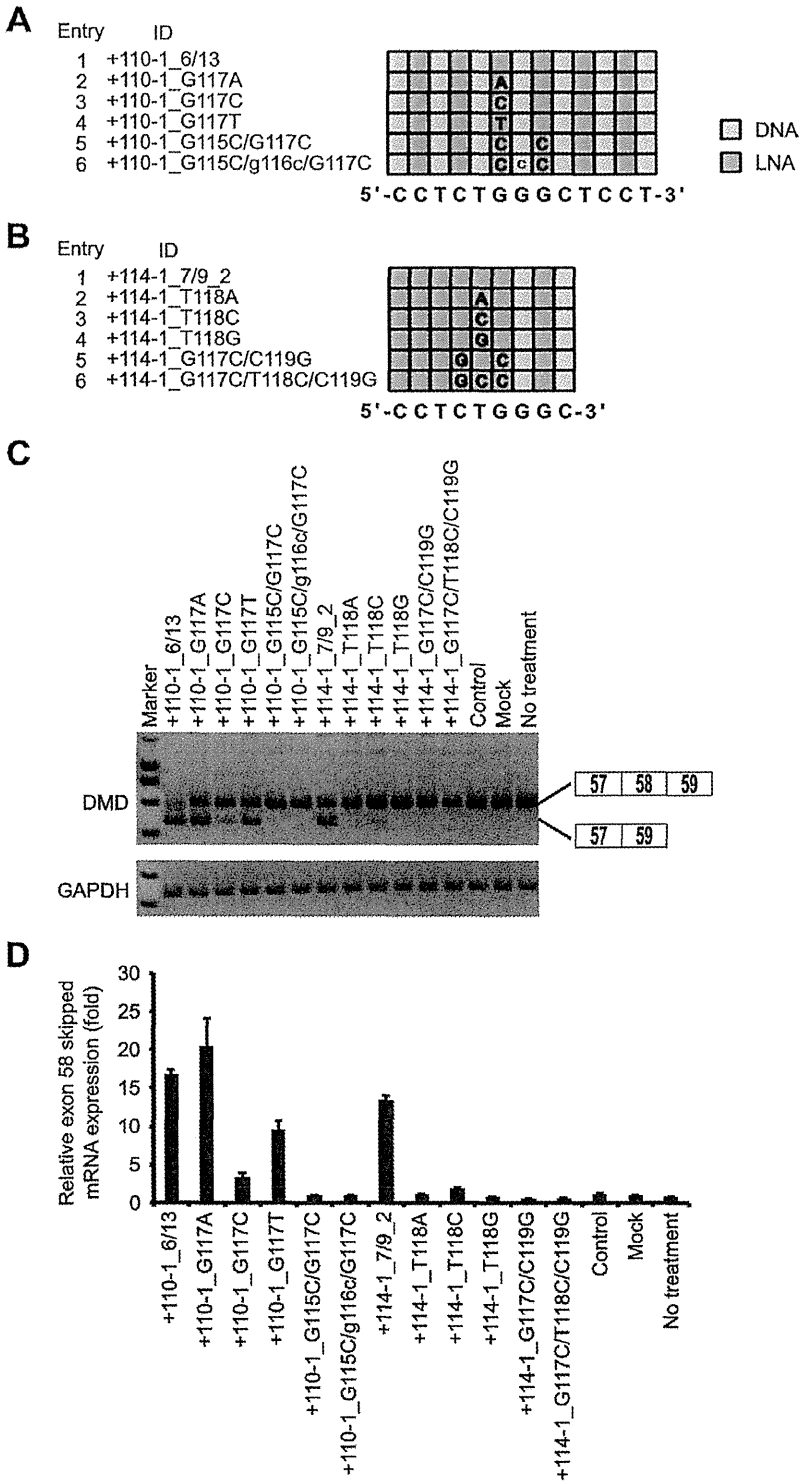

Figure 7. Assessment of specificity of LNA SSO. (**A** and **B**) Schematic representation of the position of LNA in the 13-mer SSOs (A) and the 9-mer SSOs (B) used in this study. The sequence in the box indicates a mismatch. Capital letter A, G, T: LNA; C: 5-methyl cytosine LNA; lowercase letter: DNA. (**C**) The reporter cells were transfected with the indicated LNA/DNA mixmer SSOs (30 nM) for 24 h. RT-PCR analyses were performed as described in Figure 3B. (**D**) The levels of exon 58-skipped mRNA fragments were measured by quantitative real-time RT-PCR (for details see Materials and Methods and Figure 2G). Values represent the mean ± standard deviation of triplicate samples. Reproducible results were obtained from two independent experiments.

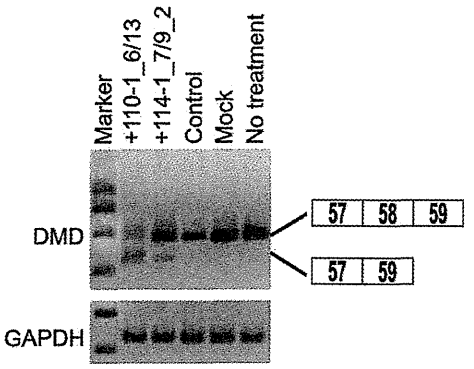

Figure 8. Exon skipping by LNA SSOs in primary human skeletal muscle cells. HSMM cells were transfected with the indicated LNA/DNA mixmer SSOs (500 nM) for 24 h. RT-PCR analyses show the full-length upper band (575 bp) and the skipped lower band (454 bp). LNA SSO (+10+24), which showed no exon skipping effects, was used as a control. GAPDH was used as an internal control.

the 2′-OMe modification resulted in an increase of only ~1°C per nucleotide incorporated (47). UV melting experiments performed under low-sodium conditions (10 mM phosphate buffer (pH 7.2) containing 10 mM NaCl) revealed that the T_m values of LNA SSO (five LNA and ten DNA) and 2′-OMe SSO (five 2′-OMe and ten DNA) were 69.5°C and 50.1°C, respectively (Supplementary Table S4). Thus, it seems that a higher melting temperature is associated with higher SSO activity. However, SSOs fully modified with LNA showed low activity despite their high T_m values. LNA-modified oligonucleotides often form stable self-structures (hairpin or self-dimer) (48). In particular, fully modified LNA SSOs might impair skipping activity because of self-dimerization, which led to decrease of effective SSO concentration for mRNA targeting (data not shown). In addition, we and others previously reported that AONs that possess very high binding affinity exhibit a relatively weak silencing ability (49,50). One of the reasons for this is that because AONs dissociated from the RNase H-dependent cleaved target mRNA could enter a new round of catalysis, LNA AONs with too high affinity might reduce the dissociation rate. Thus, LNA AONs are thought to require optimal binding affinity for efficient turnover activities in antisense reaction (51,52). Indeed, higher antisense effects were obtained by using LNA AONs whose T_m values were less than 65°C (10 mM phosphate buffer (pH 7.2) containing 100 mM NaCl) (49,50). In the case of exon skipping, SSO is also thought to be recycled after dissociation from the excised region (53). Thus, the values are different from those obtained for AONs, and there may be an optimum T_m range to design effective SSOs that incorporate LNA. To date, few studies have shown that LNA can be used in SSOs both *in vivo* and *in vitro* (17,18,19,20,21,22), and no information is available regarding the effects of the position and number of LNAs. Here, we report for the first time that SSOs fully modified with LNA have lower activity than LNA/DNA mixmer SSOs. This result may at least partially be explained by the optimization of T_m values described above and/or by the kinetics of duplex formation between LNA-based SSOs and RNA (54). Christensen reported that the rate of association of full-length LNA-based 10-mer oligonucleotides to complementary RNA was lower than that of a LNA/DNA mixmer (five LNA and five DNA) and the association constant of the full-length LNA-based oligonucleotide to complementary RNA was 1.5- to 2-fold less than that of the LNA/DNA mixmer in the presence of magnesium ions. Therefore, SSOs fully modified with LNA may be too rigid to use as splicing modulators, in contrast to LNA/DNA mixmers.

Third, our study of SSO length indicates that optimal lengths exist for LNA SSOs to modulate splicing. The quantitative real-time RT-PCR results indicated that the 13-mer SSO showed the highest effectiveness for exon skipping, whereas exon skipping activities of the above 15-mer LNA SSOs were decreased with increasing length (Figure 4). In this experiment, we used SSOs in which a LNA monomer was introduced on every other base. Therefore, longer SSOs exhibited higher binding abilities with smaller K_d values (Supplementary Table S6). These results are in good agreement with the T_m values. Thus, the decreased exon skipping activity should be brought by the other reason, such as intra- or intermolecular structures due to high number of LNAs in the SSO sequence (see above). On the other hand, in these experiments, all SSOs had a PS backbone in their sequence to provide nuclease resistance (55). Although the PS backbone decreases the T_m by ~1°C per substitution (56,57), the PS-LNA oligonucleotides have still high T_m values due to high affinity of LNA for the complementary RNA (Supplementary Tables S4 and S5) (58). Thus, PS backbone did not influence the binding affinity of PS-LNA SSO toward complementary RNA very much. Taken together, these ideas may explain why shorter LNA SSOs showed high splicing activity, and why 13-mer LNA/DNA SSO mixmers had the highest effectiveness for exon skipping.

Although Ittig *et al.* showed that a 9-mer fully modified LNA SSO has no significant exon skipping effect (20), we here demonstrated, for the first time, that LNA SSOs as short as 7 mers have the potential to modulate splicing in a concentration-dependent manner provided that they are highly modified and display high T_m values (Figures 5 and 6). Shorter SSOs may have a further advantage in that the production costs of oligonucleotide drugs are higher than that of small molecules; therefore, shorter oligonucleotides may provide a cost-effective solution to the development of oligonucleotide drugs. Although, the activity of the 9-mer SSO (four LNA and five DNA) was weaker than that of the 13-mer SSO, quantitative real-time RT-PCR experiments revealed that the expression of skipped mRNA was similar among 9-, 19-, 21- and 23-mer SSOs (Figure 4). Intriguingly, when we compared two 9-mer LNA/DNA mixmer SSOs containing seven LNA analogues at different positions in each sequence, one of them presented 1.5-fold higher activity than the other despite their similar T_m values (87.1°C and 83.1°C) (Supplementary Table S7). Thus, the position of LNA analogues in the SSO sequence may be an important factor for exon skipping. Of note, the 9-mer 2′-OMe SSO (four 2′-OMe and five DNA), which has a low T_m value (40.0°C), exhibited no exon skipping activity at all (Figure 5).

Kandimalla *et al.* reported that short oligonucleotides (9-mers) bind more specifically than longer oligonucleotides (such as 21-mers), possibly because longer oligonucleotides have a higher chance of binding to various target sequences containing up to two mismatches than do short oligonucleotides, given the sufficient T_m values of longer oligonucleotides for forming duplexes with mismatched sequences (59). Indeed, Guterstam *et al.* demonstrated that the 18-mer PS LNA/2'-OMe mixmers with four mismatches, including one LNA mismatch, induced exon skipping (17). On the other hand, Obad *et al.* reported that 8-mer LNAs, termed tiny LNAs, inhibit microRNA activity without off-target effects (60). In this study, we evaluated the sequence specificity of LNA/DNA mixmer SSOs by introducing mismatches. The 13-mer LNA SSO (+110-1_6/13) containing one LNA mismatch was able to induce exon skipping, while the exon skipping activity is abolished when one to three LNA mismatches are introduced in the center of the 9-mer LNA SSO (+114-1_7/9_2). Thus, the 9-mer LNA SSO improved mismatch discrimination in comparison with the 13-mer LNA SSO. However, in our *in silico* analysis, the number of target genes that have perfect match with 9-mer LNA SSO (+114-1_7/9_2) is far larger than that of the 13-mer LNA SSO (+110-1_6/13) (914 genes and 8 genes, respectively) (Table 1). Although the ability to discriminate between the matched and mismatched sequences is improved by shorter SSO, these results suggest that it is important to design LNA SSOs in consideration of off target-effects.

In conclusion, we found that the number of LNAs in the SSO sequence, the T_m of the SSOs and the length of the LNA SSOs are key factors for their activity. We also show for the first time that 7-mer LNA SSOs induce exon skipping. Our findings suggest that LNA SSO-mediated exon skipping may be an attractive therapeutic strategy for genetic diseases.

SUPPLEMENTARY DATA

Supplementary Data are available at NAR Online.

FUNDING

Grant-in-Aid for Exploratory Research and Project MEET, Osaka University Graduate School of Medicine. Funding for open access charge: Grant-in-Aid for Scientific Research (A).

Conflict of interest statement. None declared.

REFERENCES

1. Modrek,B. and Lee,C. (2002) A genomic view of alternative splicing. *Nat. Genet.*, **30**, 13–19.
2. Perez,B., Rincon,A., Jorge-Finnigan,A., Richard,E., Merinero,B., Ugarte,M. and Desviat,L.R. (2009) Pseudoexon exclusion by antisense therapy in methylmalonic aciduria (MMAuria). *Hum. Mutat.*, **30**, 1676–1682.
3. Cartegni,L., Chew,S.L. and Krainer,A.R. (2002) Listening to silence and understanding nonsense: exonic mutations that affect splicing. *Nat. Rev. Genet.*, **3**, 285–298.
4. Padgett,R.A. (2012) New connections between splicing and human disease. *Trends Genet.*, **28**, 147–154.
5. Hammond,S.M. and Wood,M.J. (2011) Genetic therapies for RNA mis-splicing diseases. *Trends Genet.*, **27**, 196–205.
6. Spitali,P. and Aartsma-Rus,A. (2012) Splice modulating therapies for human disease. *Cell*, **148**, 1085–1088.
7. Wahl,M.C., Will,C.L. and Luhrmann,R. (2009) The spliceosome: design principles of a dynamic RNP machine. *Cell*, **136**, 701–718.
8. Kole,R., Krainer,A.R. and Altman,S. (2012) RNA therapeutics: beyond RNA interference and antisense oligonucleotides. *Nat. Rev. Drug Discov.*, **11**, 125–140.
9. Dominski,Z. and Kole,R. (1993) Restoration of correct splicing in thalassemic pre-mRNA by antisense oligonucleotides. *Proc. Natl. Acad. Sci. U. S. A.*, **90**, 8673–8677.
10. Saleh,A.F., Arzumanov,A.A. and Gait,M.J. (2012) Overview of alternative oligonucleotide chemistries for exon skipping. *Methods Mol. Biol.*, **867**, 365–378.
11. Yamamoto,T., Nakatani,M., Narukawa,K. and Obika,S. (2011) Antisense drug discovery and development. *Future Med. Chem.*, **3**, 339–365.
12. Singh,S.K., Nielsen,P., Koshkin,A.A. and Wengel,J. (1998) LNA (locked nucleic acids): synthesis and high-affinity nucleic acid recognition. *Chem. Commun.*, **4**, 455–456.
13. Obika,S., Nanbu,D., Hari,Y., Morio,K., In,Y., Ishida,T. and Imanishi,T. (1997) Synthesis of 2'-O,4'-C-methyleneuridine and -cytidine. Novel bicyclic nucleosides having a fixed C-3,-endo sugar puckering. *Tetrahedron Lett.*, **38**, 8735–8738.
14. Braasch,D.A. and Corey,D.R. (2001) Locked nucleic acid (LNA): fine-tuning the recognition of DNA and RNA. *Chem. Biol.*, **8**, 1–7.
15. Bondensgaard,K., Petersen,M., Singh,S.K., Rajwanshi,V.K., Kumar,R., Wengel,J. and Jacobsen,J.P. (2000) Structural studies of LNA:RNA duplexes by NMR: conformations and implications for RNase H activity. *Chemistry*, **6**, 2687–2695.
16. Vester,B. and Wengel,J. (2004) LNA (locked nucleic acid): high-affinity targeting of complementary RNA and DNA. *Biochemistry*, **43**, 13233–13241.
17. Guterstam,P., Lindgren,M., Johansson,H., Tedebark,U., Wengel,J., El Andaloussi,S. and Langel,U. (2008) Splice-switching efficiency and specificity for oligonucleotides with locked nucleic acid monomers. *Biochem. J.*, **412**, 307–313.
18. Aartsma-Rus,A., Kaman,W.E., Bremmer-Bout,M., Janson,A.A., den Dunnen,J.T., van Ommen,G.J. and van Deutekom,J.C. (2004) Comparative analysis of antisense oligonucleotide analogs for targeted DMD exon 46 skipping in muscle cells. *Gene Ther.*, **11**, 1391–1398.
19. Graziewicz,M.A., Tarrant,T.K., Buckley,B., Roberts,J., Fulton,L., Hansen,H., Orum,H., Kole,R. and Sazani,P. (2008) An endogenous TNF-alpha antagonist induced by splice-switching oligonucleotides reduces inflammation in hepatitis and arthritis mouse models. *Mol. Ther.*, **16**, 1316–1322.
20. Ittig,D., Liu,S., Renneberg,D., Schumperli,D. and Leumann,C.J. (2004) Nuclear antisense effects in cyclophilin A pre-mRNA splicing by oligonucleotides: a comparison of tricyclo-DNA with LNA. *Nucleic Acids Res.*, **32**, 346–353.
21. Roberts,J., Palma,E., Sazani,P., Orum,H., Cho,M. and Kole,R. (2006) Efficient and persistent splice switching by systemically delivered LNA oligonucleotides in mice. *Mol. Ther.*, **14**, 471–475.
22. Yilmaz-Elis,A.S., Aartsma-Rus,A., t Hoen,P.A., Safdar,H., Breukel,C., van Vlijmen,B.J., van Deutekom,J., de Kimpe,S., van Ommen,G.J. and Verbeek,J.S. (2013) Inhibition of IL-1 Signaling by antisense oligonucleotide-mediated exon skipping of IL-1 receptor accessory protein (IL-1RAcP). *Mol. Ther. Nucleic Acids*, **2**, e66.
23. Goemans,N.M., Tulinius,M., van den Akker,J.T., Burm,B.E., Ekhart,P.F., Heuvelmans,N., Holling,T., Janson,A.A., Platenburg,G.J., Sipkens,J.A. *et al.* (2011) Systemic administration of PRO051 in Duchenne's muscular dystrophy. *N. Engl. J. Med.*, **364**, 1513–1522.
24. van Deutekom,J.C., Janson,A.A., Ginjaar,I.B., Frankhuizen,W.S., Aartsma-Rus,A., Bremmer-Bout,M., den Dunnen,J.T., Koop,K., van der Kooi,A.J., Goemans,N.M. *et al.* (2007) Local dystrophin restoration with antisense oligonucleotide PRO051. *N. Engl. J. Med.*, **357**, 2677–2686.
25. Morita,K., Hasegawa,C., Kaneko,M., Tsutsumi,S., Sone,J., Ishikawa,T., Imanishi,T. and Koizumi,M. (2002) 2'-O,4'-C-ethylene-bridged nucleic acids (ENA): highly nuclease-resistant and thermodynamically stable oligonucleotides for antisense drug. *Bioorg. Med. Chem. Lett.*, **12**, 73–76.

26. Cirak,S., Arechavala-Gomeza,V., Guglieri,M., Feng,L., Torelli,S., Anthony,K., Abbs,S., Garralda,M.E., Bourke,J., Wells,D.J. *et al.* (2011) Exon skipping and dystrophin restoration in patients with Duchenne muscular dystrophy after systemic phosphorodiamidate morpholino oligomer treatment: an open-label, phase 2, dose-escalation study. *Lancet*, **378**, 595–605.
27. Kinali,M., Arechavala-Gomeza,V., Feng,L., Cirak,S., Hunt,D., Adkin,C., Guglieri,M., Ashton,E., Abbs,S., Nihoyannopoulos,P. *et al.* (2009) Local restoration of dystrophin expression with the morpholino oligomer AVI-4658 in Duchenne muscular dystrophy: a single-blind, placebo-controlled, dose-escalation, proof-of-concept study. *Lancet Neurol.*, **8**, 918–928.
28. Mendell,J.R., Rodino-Klapac,L.R., Sahenk,Z., Roush,K., Bird,L., Lowes,L.P., Alfano,L., Gomez,A.M., Lewis,S., Kota,J. *et al.* (2013) Eteplirsen for the treatment of Duchenne muscular dystrophy. *Ann. Neurol.*, **74**, 637–647.
29. Muntoni,F. and Wood,M.J. (2011) Targeting RNA to treat neuromuscular disease. *Nat. Rev. Drug Discov.*, **10**, 621–637.
30. Aartsma-Rus,A. (2012) Overview on AON design. *Methods Mol. Biol.*, **867**, 117–129.
31. Aartsma-Rus,A., van Vliet,L., Hirschi,M., Janson,A.A., Heemskerk,H., de Winter,C.L., de Kimpe,S., van Deutekom,J.C., t Hoen,P.A. and van Ommen,G.J. (2009) Guidelines for antisense oligonucleotide design and insight into splice-modulating mechanisms. *Mol. Ther.*, **17**, 548–553.
32. Orengo,J.P., Bundman,D. and Cooper,T.A. (2006) A bichromatic fluorescent reporter for cell-based screens of alternative splicing. *Nucleic Acids Res.*, **34**, e148.
33. Rozen,S. and Skaletsky,H. (2000) Primer3 on the WWW for general users and for biologist programmers. *Methods Mol. Biol.*, **132**, 365–386.
34. Wu,B., Benrashid,E., Lu,P., Cloer,C., Zillmer,A., Shaban,M. and Lu,Q.L. (2011) Targeted skipping of human dystrophin exons in transgenic mouse model systemically for antisense drug development. *PLoS One*, **6**, e19906.
35. Naito,Y. and Bono,H. (2012) GGRNA: an ultrafast, transcript-oriented search engine for genes and transcripts. *Nucleic Acids Res.*, **40**, W592–W596.
36. Kurreck,J., Wyszko,E., Gillen,C. and Erdmann,V.A. (2002) Design of antisense oligonucleotides stabilized by locked nucleic acids. *Nucleic Acids Res.*, **30**, 1911–1918.
37. Cartegni,L., Wang,J., Zhu,Z., Zhang,M.Q. and Krainer,A.R. (2003) ESEfinder: a web resource to identify exonic splicing enhancers. *Nucleic Acids Res.*, **31**, 3568–3571.
38. Smith,P.J., Zhang,C., Wang,J., Chew,S.L., Zhang,M.Q. and Krainer,A.R. (2006) An increased specificity score matrix for the prediction of SF2/ASF-specific exonic splicing enhancers. *Hum. Mol. Genet.*, **15**, 2490–2508.
39. Warf,M.B. and Berglund,J.A. (2009) Role of RNA structure in regulating pre-mRNA splicing. *Trends Biochem. Sci.*, **35**, 169–178.
40. Aartsma-Rus,A., Fokkema,I., Verschuuren,J., Ginjaar,I., van Deutekom,J., van Ommen,G.J. and den Dunnen,J.T. (2009) Theoretic applicability of antisense-mediated exon skipping for Duchenne muscular dystrophy mutations. *Hum. Mutat.*, **30**, 293–299.
41. Pozzoli,U., Elgar,G., Cagliani,R., Riva,L., Comi,G.P., Bresolin,N., Bardoni,A. and Sironi,M. (2003) Comparative analysis of vertebrate dystrophin loci indicate intron gigantism as a common feature. *Genome Res.*, **13**, 764–772.
42. Wilton,S.D., Fall,A.M., Harding,P.L., McClorey,G., Coleman,C. and Fletcher,S. (2007) Antisense oligonucleotide-induced exon skipping across the human dystrophin gene transcript. *Mol. Ther.*, **15**, 1288–1296.
43. Aartsma-Rus,A., De Winter,C.L., Janson,A.A., Kaman,W.E., Van Ommen,G.J., Den Dunnen,J.T. and Van Deutekom,J.C. (2005) Functional analysis of 114 exon-internal AONs for targeted DMD exon skipping: indication for steric hindrance of SR protein binding sites. *Oligonucleotides*, **15**, 284–297.
44. Aartsma-Rus,A., Houlleberghs,H., van Deutekom,J.C., van Ommen,G.J. and t Hoen,P.A. (2010) Exonic sequences provide better targets for antisense oligonucleotides than splice site sequences in the modulation of Duchenne muscular dystrophy splicing. *Oligonucleotides*, **20**, 69–77.
45. Koshkin,A.A., Singh,S.K., Nielsen,P., Rajwanshi,V.K., Kumar,R., Meldgaard,M., Olsen,C.E. and Wengel,J. (1998) LNA (Locked Nucleic Acids): synthesis of the adenine, cytosine, guanine, 5-methylcytosine, thymine and uracil bicyclonucleoside monomers, oligomerisation, and unprecedented nucleic acid recognition. *Tetrahedron*, **54**, 3607–3630.
46. Obika,S., Nanbu,D., Hari,Y., Andoh,J., Morio,K., Doi,T. and Imanishi,T. (1998) Stability and structural features of the duplexes containing nucleoside analogues with a fixed N-type conformation, 2 '-O,4 '-C-methyleneribonucleosides. *Tetrahedron Lett.*, **39**, 5401–5404.
47. Lesnik,E.A., Guinosso,C.J., Kawasaki,A.M., Sasmor,H., Zounes,M., Cummins,L.L., Ecker,D.J., Cook,P.D. and Freier,S.M. (1993) Oligodeoxynucleotides containing 2'-O-modified adenosine: synthesis and effects on stability of DNA:RNA duplexes. *Biochemistry*, **32**, 7832–7838.
48. Lennox,K.A. and Behlke,M.A. (2011) Chemical modification and design of anti-miRNA oligonucleotides. *Gene Ther.*, **18**, 1111–1120.
49. Yamamoto,T., Yasuhara,H., Wada,F., Harada-Shiba,M., Imanishi,T. and Obika,S. (2012) Superior silencing by 2',4'-BNA(NC)-based short antisense oligonucleotides compared to 2',4'-BNA/LNA-based apolipoprotein B antisense inhibitors. *J. Nucleic Acids*, **2012**, 707323.
50. Straarup,E.M., Fisker,N., Hedtjarn,M., Lindholm,M.W., Rosenbohm,C., Aarup,V., Hansen,H.F., Orum,H., Hansen,J.B. and Koch,T. (2010) Short locked nucleic acid antisense oligonucleotides potently reduce apolipoprotein B mRNA and serum cholesterol in mice and non-human primates. *Nucleic Acids Res.*, **38**, 7100–7111.
51. Yamamoto,T., Fujii,N., Yasuhara,H., Wada,S., Wada,F., Shigesada,N., Harada-Shiba,M. and Obika,S. (2014) Evaluation of multiple-turnover capability of locked nucleic acid antisense oligonucleotides in cell-free RNase H-mediated antisense reaction and in mice. *Nucleic Acid Ther.*, 10.1089/nat.2013.0470.
52. Pedersen,L., Hagedorn,P.H., Lindholm,M.W. and Lindow,M. (2014) A kinetic model explains why shorter and less affine enzyme-recruiting oligonucleotides can be more potent. *Mol. Ther. Nucleic Acids*, **3**, e149.
53. Sierakowska,H., Sambade,M.J., Agrawal,S. and Kole,R. (1996) Repair of thalassemic human beta-globin mRNA in mammalian cells by antisense oligonucleotides. *Proc. Natl. Acad. Sci. U. S. A.*, **93**, 12840–12844.
54. Christensen,U. (2007) Thermodynamic and kinetic characterization of duplex formation between 2'-O, 4'-C-methylene-modified oligoribonucleotides, DNA and RNA. *Biosci. Rep.*, **27**, 327–333.
55. Akhtar,S., Kole,R. and Juliano,R.L. (1991) Stability of antisense DNA oligodeoxynucleotide analogs in cellular extracts and sera. *Life Sci.*, **49**, 1793–1801.
56. Stein,C.A., Subasinghe,C., Shinozuka,K. and Cohen,J.S. (1988) Physicochemical properties of phosphorothioate oligodeoxynucleotides. *Nucleic Acids Res.*, **16**, 3209–3221.
57. Freier,S.M. and Altmann,K.H. (1997) The ups and downs of nucleic acid duplex stability: structure-stability studies on chemically-modified DNA:RNA duplexes. *Nucleic Acids Res.*, **25**, 4429–4443.
58. Kumar,R., Singh,S.K., Koshkin,A.A., Rajwanshi,V.K., Meldgaard,M. and Wengel,J. (1998) The first analogues of LNA (locked nucleic acids): phosphorothioate-LNA and 2'-thio-LNA. *Bioorg. Med. Chem. Lett.*, **8**, 2219–2222.
59. Kandimalla,E.R., Manning,A., Lathan,C., Byrn,R.A. and Agrawal,S. (1995) Design, biochemical, biophysical and biological properties of cooperative antisense oligonucleotides. *Nucleic Acids Res.*, **23**, 3578–3584.
60. Obad,S., dos Santos,C.O., Petri,A., Heidenblad,M., Broom,O., Ruse,C., Fu,C., Lindow,M., Stenvang,J., Straarup,E.M. *et al.* (2011) Silencing of microRNA families by seed-targeting tiny LNAs. *Nat. Genet.*, **43**, 371–378.

テネイシン抗体とα-マンゴスチンとの複合投与による乳癌転移抑制の試み

柴田雅朗[1)]・日下部守昭[2)]・森本純司[3)]・柴田映子[4)]
斯波真理子[4)]・的場吉信[5)]・土佐秀樹[6)]・飯沼宗和[7)]

[1)] 大阪保健医療大学大学院 保健医療学研究科 解剖学・病理組織学研究室
[2)] 東京大学大学院 農学生命科学研究科 食の安全研究センター [3)] 大阪医科大学 実験動物センター
[4)] 国立循環器病研究センター研究所 病態代謝部 [5)] 米田薬品工業株式会社
[6)] 株式会社フィールドアンドデバイス [7)] 岐阜薬科大学大学院 生薬学研究室

要旨

【背景】抗体医薬が効果を示す癌腫は限定的で、固形癌に対する抗腫瘍効果は十分ではない。その理由は固形癌では異常シグナル経路が複雑で、迂回路も存在するからと考えられる。

【目的】テネイシンC（TNC）抗体とマンゴスチン果皮抽出物のα-mangostinとの複合治療を行い、両者の複合により、異なった癌の増殖・転移を担うシグナル伝達経路網を標的とするアプローチを試みた。

【方法】高転移性乳癌細胞株（BJMC3879Luc2）をマウスに移植し、2週間後にTNC抗体（125μg、週2回、腹腔内投与）、α-mangostin（4000ppm, 混餌投与）並びに両者の組み合わせ投与を実施した。なお、対照群は生理食塩水のみを投与した。投与開始の6週経過後に実験を終了し、全生存動物を屠殺・剖検した。

【結果】体重では、対照群と各群との間に明らかな差異は観察されなかった。経時的な腫瘍体積では、対照群と比較して、全ての治療群で実験開始の1週より実験終了の6週まで抑制が観察された。実験終了時における生体イメージング解析では、対照群と比較して、治療群で転移の拡がりは小さい傾向にあった。病理組織学的検索では、リンパ節転移および肺転移を含む総ての転移の1匹当たりの数は、対照群と比較して、全ての治療群で有意な低下が示された。また、腫瘍内のリンパ管侵襲の数も全ての治療群で有意な低下を示した。腫瘍内の血管密度では、α-mangostinと複合投与群で有意な抑制が観察された。

【結論】高転移性マウス乳癌モデルに対して、TNC抗体あるいはα-mangostinは腫瘍増殖の抑制作用と転移抑制作用を発揮したが、両者を複合することによる明らかな抗腫瘍作用の増強効果は示されなかった。

連絡先：大阪保健医療大学大学院 保健医療学研究科
〒530-0043 大阪市北区天満1丁目9番27号
Tel: 06-6352-0093 Fax: 06-6352-5995
E-mail: masaaki.shibata@ohsu.ac.jp

はじめに

International Agency for Research on Cancer（IARC）によれば、世界において2008年に乳癌と診断された患者数は1,384,000人で、その年に458,000人の女性が乳癌で死亡した[1)]。日本の国立がんセンター・がん対策情報センターの2008年統計の報告では、我が国の乳癌による死亡率は第5位で、年齢別にみた女性の乳癌の罹患率は30歳代から増加し、40歳代後半から50歳代前半にピークを迎え、その後は次第に減少傾向を示す。年次推移は罹患率、死亡率ともに増加を示し、出生年代別では最近生まれた人ほど罹患率、死亡率が高い傾向がある。罹患率の国際比較では、東アジアよりも欧米、特にアメリカ在住の白人で高く、アメリカの日本人移民では日本国内在住者より高い傾向にある[2)]。これらの動向には生活様式の欧米化がその一因と考えられており、乳癌発生率の増加は世界的な傾向にある。

テネイシンC（TNC）は細胞外マトリックスの

糖タンパク質で、4つのドメインからなり、分子量210～400kDaのサブユニットで構成されている。このサブユニットにはEGF様ドメイン、フィブロネクチンタイプIII繰り返しドメイン、フィブリノーゲン様ドメインがある。フィブロネクチンタイプIII繰り返しドメインには選択的スプライシングを受ける領域があり、分子量の異なる多様なバリアントを作り出す[3]。TNCの低分子量バリアントは正常では骨形成に関与し[4]、高分子量バリアントでは、様々な癌組織で高発現し[3]、特に乳癌ではその進展や転移にも関わっていると報告されている[5-7]。また、腫瘍細胞によるTNCの発現は腫瘍間質の血管新生をもたらし[8]、癌細胞の増殖・浸潤・転移と微小環境（癌間質）との相互作用の重要性が認識された。

マンゴスチン（学名*Garcinia mangostana* L）は東南アジアを代表するトロピカルフルーツであり、その果皮にはキサントンが豊富に含まれ、果皮が傷つくと、キサントンを含む黄色物質が分泌され、自らを細菌感染から守る。また、分泌物は昆虫の忌避物質でもあり、昆虫から果実を守る効果もある[9]。原産地に暮らす人々の間では、マンゴスチン果皮は古くから、鎮痛、皮膚病、創傷、赤痢、伝染性の下痢などの治療薬として用いられてきており、天然の薬として代々受け継がれ、重宝されてきた[9,10]。

マンゴスチン果皮に含まれる約40種類のキサントンのうち、α-およびγ-mangostinには抗菌作用、抗炎症作用、抗アレルギー作用、癌細胞に対する殺作用を有していることが科学的に証明され、その生理活性が注目されるようになった[11-13]。また、マウスやヒトでパナキサントン（α-mangostin 75～85%およびγ-mangostin 5～15%の混合物で、両者の含量総和が90%以上のもの）を摂取するとNK活性が上昇することも確認されている[13]。2009年、私達はパナキサントンがマウス乳癌に対して抗腫瘍効果を有することを報告した[14]。次いで、2011年、先の乳癌モデルに対して、α-mangostin単体でも抗腫瘍効果を発揮したことを報告し、その作用機序の一端も明らかにした[15,16]。

抗体医薬は、分子標的に結合することにより、抗腫瘍効果を示す分子標的治療である。抗体医薬が抗腫瘍効果を示す悪性疾患は白血病や悪性リンパ腫であり、固形癌に対してはその効果は必ずしも十分とは言えない[17]。その理由は固形癌では異常シグナル経路が複雑で、迂回路も存在するからと考えられる。従って、固形癌に対する抗体医薬の開発はハードルが高い。そこで、TNC抗体によりTNC分子を標的とし、またα-mangostinにより癌細胞自身を標的として、高転移性マウス乳癌モデルに対して、実験的治療を行い、さらにこれら両者の組み合わせ投与により加算的な抗腫瘍効果が得られるかどうかを検討した。

材料と方法

乳癌細胞株

本実験で用いた乳癌細胞株BJMC3879Luc2は、BALB/c系マウスにMMTVを接種することにより誘発された乳癌より樹立されたBJMC3879細胞株[18]にLuciferase遺伝子を安定的に組み込んだものである[19]。BJMC3879細胞株を同系マウスに移植するとリンパ節や肺に高率に転移を起こす[20-22]。

投与物質

TNC抗体：ヒトメラノーマ細胞株（GIT培地で培養）の培養上清から精製したTNCを抗原として、ラットに接種し、マウスのミエローマNS-1細胞と融合させたハイブリドーマから作製したラットのモノクローナル抗体である。抗体はプロテインGカラムで精製して使用した。

α-mangostin：タイ産の成熟マンゴスチン果皮を乾燥した後、粉砕し、精製水とエタノール抽出、凍結乾燥、エチルアセテート抽出、クロマトグラフィーを用いた精製を経てα-mangostin結晶を得た。純度は＞98%であった。

In vivo乳癌モデル実験

6週齢の50匹のBALB/c系雌マウス（日本SLC）の鼠径部皮下乳腺部にBJMC3879Luc2細胞を移植し、2週後に腫瘍径が0.5～0.7cm大の40匹の動物を無作為に選び、群分けした。1群は対照群で、5%コーンオイルを含むクレアCE-2粉末飼料を自由摂取させると共に、生理食塩水を週に2回、腹腔内投与した。2群は前述と同様に

CE-2粉末飼料を与え、TNC抗体125 μg（溶媒：生理食塩水）を週に2回、腹腔内投与した。3群にはα-mangostinを4000ppm濃度に混じたクレアCE-2粉末飼料（5％コーンオイル含有）を自由摂取させると共に、生理食塩水を週に2回、腹腔内投与した。4群には、4000ppmのα-マンゴスチン含有飼料を自由摂取させると共に、TNC抗体125 μgを週に2回、腹腔内投与した。毎週、体重と乳腺腫瘍のサイズを個体別に測定した。乳腺腫瘍はデジタル式キャリパスで短径と長径を計測し、その体積を長径×（短径）^{2}×0.4の算出式で求めた[23]。実験開始の6週経過後には、全生存動物を屠殺剖検し、乳腺腫瘍を摘出し、10%リン酸緩衝ホルマリン溶液にて固定した。肺およびリンパ節(腋窩部、鼠径大腿部)を採取し、更に肉眼病変部と異常の見られたリンパ節についても採取し、病理組織学的に検索した。

癌転移の生体イメージング

実験終了の6週時に、マウス1匹当たり3 mgのD-luciferin potassium salts（和光純薬工業）を腹腔内に投与し、イソフルレン吸入麻酔下にて、Photon Imager（桑和貿易、Biospace社）を用いて、生体発光イメージングを行い、転移の拡がりを群間で比較した。

腫瘍内微小血管の定量と腫瘍内のリンパ管侵襲の数

血管内皮のマーカーであるCD31を抗CD31抗体（LabVision社）を用いて、免疫組織学的染色を施し、陽性を示した毛細血管を定量した。リンパ管内皮のマーカーであるpodoplaninを抗podoplanin抗体（AngioBio社）を用いて免疫組織学的染色を施し、拡張した毛細リンパ管内腔に癌細胞浸潤を認めたそのリンパ管の数をカウントした（リンパ管侵襲）。

統計学的解析

対照群と投与群との間の定量的データではStudentのt検定を行った。発生頻度の解析にはFisherの正確確率検定を用いた。

結　果

体重：体重では、群間に統計学的な有意差は認められなかった。なお、各群とも一般状態は良好であった。なお、実験開始の3および4週に投与に起因しない死亡例が散見され、死因も不明であったため、解析から除外した。

腫瘍体積：実験開始の1週より実験終了の6週まで、全ての投与群において、対照群と比較して、一貫して腫瘍体積は有意に低値を示した。

癌転移の生体発光イメージング：実験終了時の生体発光イメージングでは、対照群と比較して、明らかに投与群では転移の拡がりは小さい傾向にあった。

転移の病理組織学的検索：マウス1匹当たりのリンパ節の転移個数は、全ての投与群で、対照群と比較して、有意な低下が示された。肺転移では、転移巣の大きさが1 mm以上のものについて、マウス1匹当たりの数を算出した結果、全ての投与群で、対照群と比較して、有意な低下が示された。

腫瘍内の微小血管密度およびリンパ管侵襲の数：免疫組織学的染色にてCD31陽性を示した腫瘍内の微小血管を算定した。微小血管密度はα-mangostin単独投与群および複合投与群で有意な減少が示された。TNC単独投与群では減少傾向のみが示され、統計学的な差異は示されなかった。同様にリンパ管内皮のマーカーであるpodoplaninを免疫組織学的に染色し、リンパ管を鑑別したところ、拡張した毛細リンパ管内腔に浸潤した癌細胞が観察された。その癌細胞の侵襲を受けたリンパ管をリンパ管侵襲の数として算定した結果、全ての投与群で有意な低下が観察された。

考　察

ヒトと類似の転移スペクトラムを有する高転移性マウス乳癌モデルに対して、TNC抗体および食餌性のα-mangostinは腫瘍増殖を低下させ、さらにリンパ節転移、肺転移のみならず全身の総ての転移を有意に抑制した。また、癌細胞の浸潤を受けた腫瘍内のリンパ管侵襲の数はTNC抗体群およびα-mangostin群で有意に抑制され、この事実はこれらの群のリンパ節転移の抑制を裏付ける所見であると考えられた。

ヒトの乳癌は主にリンパ節、肺、肝臓および骨

に転移し、殆どの場合、転移により死に至る。癌転移を克服することこそが延命効果につながると考えられ、癌治療の最大の課題と言える。本実験において、TNC抗体やα-mangostinが乳癌転移を抑制した事実は極めて臨床的に意義があると考えられる。また、ヒト乳癌ではサイズが4cmを超えると再発や転移のリスクが著しく高まることが報告されていることからも[24]、これら両群においての腫瘍サイズが、対照群のそれより小さいことは意義深い所見と考えられる。

TNCは、当初、乳癌の間質マーカーとして報告された[25]。引き続き、TNCは正常の乳管周囲や良性の乳腺腫瘍でも発現することが示され[26]、後にTNCの高分子量バリアントは乳癌で高発現し[27]、その進展や転移に関わっていると報告された[5,6,27]。また、マウス角膜損傷モデルにおいて、熱傷により誘導される血管新生を、TNCを抑制させることにより有意に減弱させたことが示された[28]。さらに、癌においては、間質から分泌されるTNCによりVEGF-Aを誘導し、血管新生をもたらすことが報告された[8]。本実験においては、TNC抗体群で腫瘍内の血管新生は対照群と比較し、低下傾向を示したが、統計学的にはP値が0.07の境界値で、有意差を示さなかった。この他にもTNCは免疫系を調節しており、種々のサイトカインや免疫担当細胞を炎症部位や損傷部位[28,29]、あるいは癌組織[30]に動員することが知られており、癌細胞の増殖・浸潤・転移と微小環境（ニッチェ）との相互作用の重要性が認識されている。

マンゴスチンは東南アジアを代表する果実で、その果皮は古くから、様々な疾患の治療薬として代々受け継がれ、民族伝承薬物として重宝されてきた。マンゴスチン果皮に含まれるα-ならびにγ-mangostinは様々な生理活性をもたらすことが報告されている。特に、α-mangostinがミトコンドリア経路によるアポトーシス誘導、細胞周期のG1期停止やS期抑制、血管新生の抑制、Akt脱リン酸化を惹起し、これらの作用の総和として抗腫瘍効果（腫瘍増殖ならびに転移の抑制）が発揮されたものと考えられた[15]。Aktはセリン／スレオニンキナーゼで、Aktが活性化するためにはThr308部位とSer473部位の両者がリン酸化されることが必要であり、PI3キナーゼの下流で制御されている[31]。Aktが活性化すると、細胞増殖、細胞生存（抗アポトーシス）、脈管新生、細胞周期などの癌の進展に関わる変化を惹起する[32]。つまり、α-mangostinの抗腫瘍効果にはAktのリン酸化抑制作用が大いに関わっているものと推察される。しかし、それに留まらず、α-mangostinには免疫活性化作用（NK活性化）、抗酸化作用、アロマターゼ抑制作用など極めて多様な効果をもたらすことから、本実験において観察されたα-mangostinの抗腫瘍効果はこれらの加算的あるいは相乗的作用の結果と言えるであろう。

最近、分子標的治療が潮流であるが、分子標的の数が一つではなく、複数の分子標的を有する治療の方が効果は高いと考えられる。α-mangostinは多岐にわたるカスケードに影響を与える薬剤であり、かつ標的性の異なるTNC抗体との複合投与を行った。しかしながら、両者の複合投与により抗腫瘍効果の増強作用が観察されるには至らなかった。その理由として、おそらく、それぞれの単独投与で、抗腫瘍効果に起因する経路が最大に修飾された結果と推測される。

以上、高転移性マウス乳癌モデルにおいて、TNC抗体およびα-mangostinは抗腫瘍効果を発揮し、特にリンパ節をはじめとする転移の抑制は臨床的意義が極めて高い所見と考えられた。今後、より複数の分子標的性を示すその他の組み合わせ投与を実施して、転移阻止に向けた研究が必要と考える。将来的に、分子標的治療は、単一な分子標的から複数の分子標的に変遷してゆくかもしれない。

謝辞ほか

本研究は、文科省の科学研究費基盤(C)(2)（課題番号24591924：柴田雅朗）の助成により実施された。なお、本研究成果を取りまとめた原著論文は執筆中であるため、詳細なデータを割愛して、Outlineの記述に限定させて頂いた。

文 献

1. International Agency Research on Cancer: Globocan 2008. http://www-dep.iarc.fr/: (5 November 2013, date last accessed) 2008
2. がん対策情報センター：日本最新がん統計まとめ（2008年）http://ganjoho.ncc.go.jp/public/statistics/pub/statistics01.html: 2010
3. Midwood, K. S. et al.: Advances in tenascin-C biology: Cell Mol Life Sci 68: 3175-99, 2011
4. Mackie, E. J. and Tucker, R. P.: Tenascin in bone morphogenesis: expression by osteoblasts and cell type-specific expression of splice variants: J Cell Sci 103 (Pt 3) : 765-71, 1992
5. Adams, M. et al.: Changes in tenascin-C isoform expression in invasive and preinvasive breast disease: Cancer Res 62: 3289-97, 2002
6. Hancox, R. A. et al.: Tumour-associated tenascin-C isoforms promote breast cancer cell invasion and growth by matrix metalloproteinase-dependent and independent mechanisms: Breast Cancer Res 11: R24, 2009
7. Guttery, D. S. et al.: Expression of tenascin-C and its isoforms in the breast: Cancer Metastasis Rev 29: 595-606, 2010
8. Tanaka, K. et al.: Tenascin-C regulates angiogenesis in tumor through the regulation of vascular endothelial growth factor expression: Int J Cancer 108: 31-40, 2004
9. Shibata, M. A. et al.: Effects of mangosteen pericarp extracts against mammary cancer: Altern Integ Med 2: 8, 2013
10. Wexler, B.: Mangosteen. Fruits of Paradise. Woodland Publishing, 2007
11. Iinuma, M. et al.: Antibacterial activity of xanthones from guttiferaeous plants against methicillin-resistant Staphylococcus aureus: J Pharm Pharmacol 48: 861-865, 1996
12. Itoh, T. et al.: Inhibitory effect of xanthones isolated from the pericarp of Garcinia mangostana L. on rat basophilic leukemia RBL-2H3 cell degranulation: Bioorg Med Chem 16: 4500-8, 2008
13. Akao, Y. et al.: Anti-cancer effects of xanthones from pericarps of mangosteen: Int J Mol Sci 9: 355-70, 2008
14. Doi, H. et al.: Panaxanthone isolated from pericarp of Garcinia mangostana L. suppresses tumor growth and metastasis of a mouse model of mammary cancer: Anticancer Res 29: 2485-95, 2009
15. Shibata, M. A. et al.: α-Mangostin extracted from the pericarp of the mangosteen (*Garcinia mangostana* Linn) reduces tumor growth and lymph node metastasis in an immunocompetent xenograft model of metastatic mammary cancer carrying a p53 mutation: BMC Med 9: 69, 2011
16. Kurose, H. et al.: Alterations in cell cycle and induction of apoptotic cell death in breast cancer cells treated with α-mangostin extracted from mangosteen pericarp: J Biomed Biotechnol 2012: 672428, 2012
17. 設樂研也：がんの抗体医薬の現状と将来，実験医学増刊 27: 49-55, 2009
18. Morimoto, J. et al.: New murine mammary tumor cell lines: In vitro Cell Dev Biol 27A: 349-351, 1991
19. Shibata, M. A. et al.: An immunocompetent murine model of metastatic mammary cancer accessible to bioluminescence imaging: Anticancer Res 29: 4389-4396, 2009
20. Shibata, M. A. et al.: Suppression of murine mammary carcinoma growth and metastasis by HSV*tk*/GCV gene therapy using *in vivo* electroporation: Cancer Gene Ther 9: 16-27, 2002
21. Shibata, M. A. et al.: Lovastatin inhibits

tumor growth and lung metastasis in mouse mammary carcinoma model: a p53-independent mitochondrial-mediated apoptotic mechanism: Carcinogenesis 25: 1887-1898, 2004

22. Shibata, M. A. et al.: Electrogene therapy using endostatin, with or without suicide gene therapy, suppresses murine mammary tumor growth and metastasis: Cancer Gene Ther 14: 268-278, 2007
23. Shibata, M. A. et al.: Haploid loss of bax leads to accelerated mammary tumor development in C3 (1) /SV40-TAg transgenic mice: reduction in protective apoptotic response at the preneoplastic stage: EMBO J. 18: 2692-2701, 1999
24. Carter, C. L. et al.: Relation of tumor size, lymph node status, and survival in 24,740 breast cancer cases: Cancer 63: 181-187, 1989
25. Mackie, E. J. et al.: Tenascin is a stromal marker for epithelial malignancy in the mammary gland: Proc Natl Acad Sci U S A 84: 4621-5, 1987
26. Howeedy, A. A. et al.: Differential distribution of tenascin in the normal, hyperplastic, and neoplastic breast: Lab Invest 63: 798-806, 1990
27. Tsunoda, T. et al.: Involvement of large tenascin-C splice variants in breast cancer progression: Am J Pathol 162: 1857-67, 2003
28. Sumioka, T. et al.: Impaired angiogenic response in the cornea of mice lacking tenascin C: Invest Ophthalmol Vis Sci 52: 2462-7, 2011
29. Midwood, K. et al.: Tenascin-C is an endogenous activator of Toll-like receptor 4 that is essential for maintaining inflammation in arthritic joint disease: Nat Med 15: 774-80, 2009
30. Talts, J. F. et al.: Tenascin-C modulates tumor stroma and monocyte/macrophage recruitment but not tumor growth or metastasis in a mouse strain with spontaneous mammary cancer: J Cell Sci 112 (Pt 12) : 1855-64, 1999
31. Bellacosa, A. et al.: Akt activation by growth factors is a multiple-step process: the role of the PH domain: Oncogene 17: 313-25, 1998
32. Agarwal, A. et al.: The AKT/I kappa B kinase pathway promotes angiogenic/metastatic gene expression in colorectal cancer by activating nuclear factor-kappa B and beta-catenin: Oncogene 24: 1021-31, 2005